Elevation gradients of European climate change in the regional climate model COSMO-CLM

Author(s):
Kotlarski, S.; Bosshard, T.; Luthi, D.; Pall, P.; Schar, C.

Publication date:
2012-05

Permanent link:
https://doi.org/10.3929/ethz-b-000048515

Originally published in:
Climatic Change 112(2), https://doi.org/10.1007/s10584-011-0195-5

Climatic Change (2012) 112:189–215
DOI 10.1007/s10584-011-0195-5

Elevation gradients of European climate change in the regional climate model COSMO-CLM

S. Kotlarski · T. Bosshard · D. Lüthi · P. Pall · C. Schär

Received: 17 January 2011 / Accepted: 28 July 2011 / Published online: 23 August 2011

Abstract A transient climate scenario experiment of the regional climate model COSMO-CLM is analyzed to assess the elevation dependency of 21st century European climate change. A focus is put on near-surface conditions. Model evaluation reveals that COSMO-CLM is able to approximately reproduce the observed altitudinal variation of 2 m temperature and precipitation in most regions and most seasons. The analysis of climate change signals suggests that 21st century climate change might considerably depend on elevation. Over most parts of Europe and in most seasons, near-surface warming significantly increases with elevation. This is consistent with the simulated changes of the free-tropospheric air temperature, but can only be fully explained by taking into account regional-scale processes involving the land surface. In winter and spring, the anomalous high-elevation warming is typically connected to a decrease in the number of snow days and the snow-albedo feedback. Further factors are changes in cloud cover and soil moisture and the proximity of low-elevation regions to the sea. The amplified warming at high elevations becomes apparent during the first half of the 21st century and results in a general decrease of near-surface lapse rates. It does not imply an early detection potential of large-scale temperature changes. For precipitation, only few consistent signals arise. In many regions precipitation changes show a pronounced elevation dependency but the details strongly depend on the season and the region under consideration. There is a tendency towards a larger relative decrease of summer precipitation at low elevations, but there are exceptions to this as well.

1 Introduction

Both anthropogenic climate change and natural climate variability are subject to pronounced spatial variations and can show distinct three-dimensional patterns. Observed past and projected future changes of near-surface air temperature, for instance, exhibit a

Electronic supplementary material The online version of this article (doi:10.1007/s10584-011-0195-5) contains supplementary material, which is available to authorized users.

S. Kotlarski (✉) · T. Bosshard · D. Lüthi · P. Pall · C. Schär
Institute for Atmospheric and Climate Science, ETH Zurich, Universitätstrasse 16, CH-8092 Zürich, Switzerland
e-mail: sven.kotlarski@env.ethz.ch

strong variability on hemispheric to regional scales and are poorly characterized by a single global mean change. Indeed, during the 20th century global mean temperature increased, but a few isolated regions experienced a slight near-surface cooling (IPCC 2007). Differences between future global mean changes and the response in individual regions can also be expected for the 21st century. This is especially true for parameters like precipitation, which strongly depend on a suite of non-linear, interacting processes that in turn are subject to a high spatial variability.

A particularly important variation of this type is the elevation dependency of surface climate change, i.e., the relation between the change of a near-surface quantity and the topographic height of the respective station or model grid cell.[1] Assessing and understanding elevation gradients and the corresponding amplification/attenuation of large-scale climate change signals in mountain regions is of high interest for climate impact assessment, given the high vulnerability of alpine ecosystems (e.g., Diaz et al. 2003, Schröter et al. 2005, Thuiller et al. 2005), the importance of mountain regions as "water towers" for the surrounding lowlands (e.g., Viviroli et al. 2007), the high frequency of heavy precipitation events and floods in regions of complex topography (e.g., Frei et al. 2000), and the role of mountains as tourist destinations (e.g., EEA 2009, Elsasser and Bürki 2002).

Recently, altitudinal climatic gradients have been investigated for a large number of mountain ranges (e.g., the reviews of Barry 2008, Schär et al. 1998). For temperature, the altitude gradient is strongly determined by the respective height gradient in the free troposphere, and it thus exhibits the prevailing environmental lapse rate (decrease of the free-tropospheric temperature with height) modulated by local conditions. Temperature height and altitude gradients are typically confined by the saturated and the dry adiabatic lapse rates of about 0.4 and 0.98°C $(100\ m)^{-1}$, respectively, but show distinct spatial, seasonal, synoptic and diurnal variations in alpine terrain (e.g., Kotlarski et al. 2010, Minder et al. 2010, Prömmel et al. 2010, Richner and Phillips 1984, Rolland 2003, Schwarb 2000, Varney 1920). Often, such variability is neglected and a mean lapse rate around 0.65°C $(100\ m)^{-1}$ is assumed as a rule of thumb. Topography also exerts a primary control on precipitation sums (e.g., Daly et al. 1994, Frei and Schär 1998, Wastl and Zängl 2008). The underlying mechanisms depend on the mountain range under consideration. They can include processes such as orographically forced uplift and orographic triggering of summertime convection, and may also involve the seeder-feeder type precipitation enhancement (e.g., Houze 1993, Roe 2005, Smith 1979). These mechanisms typically lead to an increase of precipitation amounts with elevation that is approximately linear in many regions. Exceptions are tropical and subtropical mountain ranges where maximum precipitation rates often occur at medium elevations (Daly et al. 1994, Weischet 1979). Furthermore, the complexity of orographic precipitation processes leads to a pronounced spatial heterogeneity of the precipitation-elevation gradient with distinct spatio-temporal patterns (e.g., Frei and Schär 1998, Sevruk 1997, Wastl and Zängl 2007). Elevation gradients of temperature and precipitation, in turn, strongly determine the gradients of snow

[1] For clarity, we will reserve the terms *elevation/altitude dependency* and *elevation/altitude gradient* for the altitudinal dependency of near-surface parameters, while the term *height dependency* will be reserved for variations in the free troposphere. Similarly, the term *(surface) lapse rate* will refer to the elevation dependency of *near-surface* air temperature as opposed to the *environmental lapse rate* in the free troposphere. Lapse rates are generally defined as the temperature decrease with elevation/height and hence positive in sign for cooler conditions at higher levels. In contrast, positive precipitation gradients denote an increase of precipitation with height.

accumulation and snow melt, resulting in a general increase of snow depth and snow duration with altitude (e.g., Durand et al. 2009, Hantel et al. 2000, Laternser 2002). Snow cover feedbacks are thus among the most suspicious factors when considering local changes in temperature-altitude relations. Also components of the surface radiation budget can show a pronounced altitudinal dependency (Marty et al. 2002).

Concerning future climate change, any modification of the processes determining the vertical gradients of surface climate can be expected to result in an elevation-dependent forcing and, eventually, in a modification of the respective elevation gradients. For the case of temperature, the relevant factors relate (i) to large-scale changes of the environmental lapse rate and (ii) to more regional effects related, e.g., to changes in snow cover. Regarding the former, theoretical considerations and climate model results suggest that climate change will lead to a decrease of free-tropospheric lapse rates (e.g., Frierson 2006), i.e., the upper troposphere will warm stronger than the lower, ultimately because the moist adiabatic lapse rate decreases with temperature (Held and Soden 2000, Santer et al. 2005, Soden and Held 2006). This change affects saturated ascending air parcels and is particularly effective in the tropics. Regarding the second, more regional effect, an obvious mechanism involving surface-atmosphere exchange processes is the snow-albedo feedback (e.g., Hall 2004): A shortening of the snow season will result in a lower surface albedo during the transition seasons and would potentially amplify a large-scale warming signal. This process will be most effective in mid- to high-altitude regions with large changes in snow cover duration. Further reasons for a possible elevation dependency of surface climate change have been proposed. For instance, high-elevation sites are more influenced by the free troposphere above the boundary layer (Beniston and Rebetez 1996, Weber et al. 1994) and are thus less affected by local factors (air pollution, frequency of inversions, anthropogenic land use changes, etc.).

Observational evidence confirms that surface temperature trends can have a strong altitudinal component (e.g., Beniston et al. 1997, Beniston and Rebetez 1996, Diaz and Bradley 1997, Seidel and Free 2003, Vuille and Bradley 2000, Weber et al. 1994, Weber et al. 1997). Most studies find stronger warming at high-elevation stations during the last decades, but this is not uniformly true (e.g., Appenzeller et al. 2008, Ceppi et al. 2010, Pepin and Losleben 2002, You et al. 2010). As regards future climate change, several studies have used high-resolution global and regional climate models driven by greenhouse gas scenarios. In a pioneering study, Giorgi et al. (1997) investigated the elevation dependency of surface climate change in the European Alps based on two regional climate model (RCM) time slice experiments for a control climate (present-day conditions) and a $2xCO_2$ scenario. They found a significant elevation dependency of the temperature change signal with a larger warming at higher elevations. In their experiment the differential warming is most pronounced in winter and spring and can clearly be attributed to the snow-albedo feedback. Besides temperature, the authors also found an elevation dependency of the changes in the absolute precipitation sums, especially during the summer season. Giorgi and colleagues also suggested the use of high-elevation temperature stations as an early detection tool for large-scale warming. This idea has, however, been questioned by Fyfe and Flato (1999). Analyzing an ensemble of climate change experiments with a coupled general circulation model (GCM) over the Rocky Mountains, they also found larger temperature changes at high elevations, again attributable to the snow-albedo feedback, but no potential for early climate change detection (similar signal-to-noise ratio at high and at low elevations). Further studies, applying both GCMs and RCMs, confirm the existence of an elevation signal especially for temperature in future climate change (Kim 2001, Leung and Ghan 1999, López-Moreno et al. 2008, Salathé et al. 2010, Snyder et al. 2002, Snyder

and Sloan 2005, Wild et al. 1997). Im et al. (2010) revealed the particular importance of surface-atmosphere feedback mechanisms in determining elevation gradients of both temperature and precipitation changes in the European Alps by using an RCM in a surrogate climate change framework (Schär et al. 1996) rather than driving it by a GCM. This approach accounts for the overall warming and moistening of the atmosphere but excludes a possible lapse-rate feedback.

The present study aims at complementing and extending the mentioned studies in several aspects. Instead of analyzing GCM or comparatively coarse-resolution RCM time slice experiments, we investigate a high-resolution GCM-driven transient climate change simulation over Europe carried out by a state-of-the-art RCM. In mountainous terrain, a high spatial resolution is particularly important in order to represent the topography and to reproduce meso-scale circulations and the related regional climate change characteristics. A focus is put on near-surface air temperature at 2 m height (hereafter simply referred to as *2 m temperature*) and precipitation, the main parameters typically applied in climate impact studies. Additionally, changes in the free-tropospheric air temperature are analyzed. Our future target period for deriving climate change signals is 2070–2099, which is compared to the reference period 1961–1990. Prior to the analysis of climate change signals, we assess the ability of the RCM to reproduce observed elevation gradients of 2 m temperature and precipitation. We then evaluate the spatial and temporal characteristics of the elevation dependency of surface climate change for the entire European continent, sub-divided into eight regions of similar climatic characteristics. Additional and supporting analyses that are not included in the main paper are provided in the *Electronic Supplementary Material* (ESM).

2 Data and methods

2.1 RCM data

The regional climate model applied in this study is COSMO-CLM (or in short CCLM; Rockel et al. 2008), the climate version of the COSMO numerical weather prediction model (Steppeler et al. 2003). CCLM is a non-hydrostatic limited-area model which numerically solves the fully compressible equations for a moist atmosphere. For representing subgrid-scale processes the model employs a number of physical parameterizations, including the Tiedtke convection scheme (Tiedtke 1989), a one-moment scheme for cloud microphysics, a δ-two-stream radiation scheme (Ritter and Geleyn 1992) and a land surface scheme with a multi-layer soil model. The latter also accounts for snow cover, which is represented by a single snow layer with a prognostic snow density and a time-dependent snow albedo. At the lateral boundaries, the large-scale forcing is imposed according to the relaxation scheme of Davies (1976). Spectral nudging is not applied in the current model setup, i.e., the RCM runs freely within the interior part of the model domain. At ETH Zurich CCLM is the successor of the limited-area model CHRM (Vidale et al. 2003) and is applied for studies of the regional water cycle, land surface-atmosphere interactions and for assessing future climate change in Europe and the related uncertainties. The model is developed and maintained by the CLM-community and proved to be able to represent the European climate in a similar quality as other regional climate models (e.g., Kotlarski et al. 2005).

We here analyze a set of CCLM experiments carried out within the frame of the European ENSEMBLES project (van der Linden and Mitchell 2009). The simulations comprise one evaluation run (CCLM-ERA40) for the period 1958–2002 driven by the

ERA40 re-analysis (Uppala et al. 2005) and one transient climate change experiment (CCLM-HadCM3) for the period 1950–2099 driven by the GCM HadCM3. The latter is a fully coupled ocean–atmosphere GCM which is operated without flux adjustments (Gordon et al. 2000). In the control period of CCLM-HadCM3 (1950–2000) observed atmospheric greenhouse gas concentrations are prescribed, while concentrations according to the SRES A1B emission scenario (Nakicenovic et al. 2000) are assumed from 2001 onward. In all experiments, CCLM was directly nested into the large-scale forcing and was operated at a spatial resolution of 0.22° on a rotated latitude-longitude grid, corresponding to a grid box size of approximately 25 km×25 km. The regional model domain encompasses the entire European continent, the Mediterranean Sea, parts of the North Atlantic and of Northern Africa (Fig. 1). Jaeger et al. (2008) carried out a detailed validation of CCLM-ERA40 on a European scale (referred to as CLM-22 therein). They found a number of substantial model biases, e.g., a warm and dry summer bias over many parts of Europe, but did not address elevation gradients.

2.2 Observational reference data

For validating the elevation dependency of 2 m temperature and precipitation in CCLM, we use the daily gridded E-OBS dataset as observational reference (Haylock et al. 2008). E-OBS covers the entire European land surface and is based on the ECA&D (*European Climate Assessment and Data*) station dataset plus more than 2000 further stations from different archives. The grid cells of the rotated 0.22° version of E-OBS exactly match the CCLM grid cells and no further interpolation is required for intercomparison. For the spatial interpolation of monthly values of temperature and precipitation, E-OBS uses three-dimensional splines explicitly taking into account the station elevation. We therefore assume that the elevation dependency of both parameters is approximately represented. For individual regions, more accurate datasets might exist which are based on a larger number

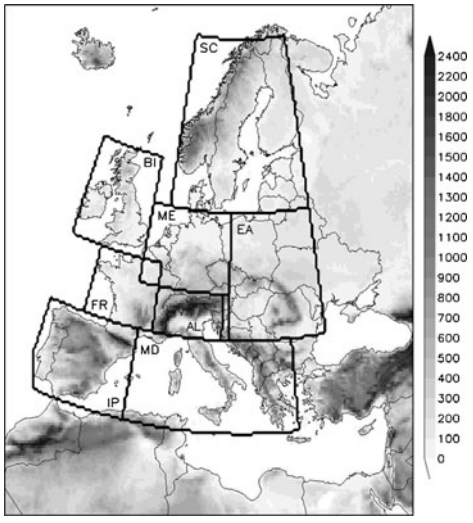

Fig. 1 CCLM model domain with grid cell orography [m] and location of the eight sub-domains (BI: British Islands, IP: Iberian Peninsula, FR: France, ME: Mid-Europe, SC: Scandinavia, AL: Alps, MD: Mediterranean, EA: Eastern Europe)

of observation stations especially at high elevations. The clear advantage of E-OBS is the spatial (entire European land surface) and temporal (1950–2006) coverage and the existence of a rotated 0.22° grid version exactly corresponding to the RCM grid, which makes it ideal for an approximate validation of the simulated elevation gradients. However, especially for the topographically structured area of the European Alps (sub-domain AL) we cannot rule out a possible bias of E-OBS towards low-elevation stations. For this sub-domain we therefore additionally consider the monthly temperature dataset of Hiebl et al. (2009) and the precipitation analysis of Schwarb et al. (2001), both of which are based on a much larger number of observation stations and provide gridded data at a higher spatial resolution than E-OBS. In their underlying measurement network more high-elevation stations are included compared to E-OBS, which does not prevent a bias of the data towards low-elevation regions (e.g., Rolland 2003) but which makes an important low-elevation bias less likely. The use of multiple observational reference datasets allows addressing observational uncertainties and increases our confidence in the model evaluation results. The 1 km×1 km temperature climatology of Hiebl et al. (2009; hereafter referred to as *ZAMG*) is provided by the *Central Institute for Meteorology and Geodynamics* (ZAMG), Austria, and has been determined from observational averages for the period 1961–1990 at 1434 stations in the greater Alpine region. The precipitation analysis of Schwarb et al. (2001; hereafter referred to as *S2001*) is based on observations of Frei and Schär (1998) at more than 6000 stations in the Alps in the period 1971–1990, which were analyzed on a 2 km grid applying the PRISM scheme (*Parameter-elevation Regression on Independent Slope Model*).

3 Methods

All analyses are carried out for annual mean values or for standard climatological seasons (DJF: winter, MAM: spring, JJA: summer, SON: autumn). Spatially, the model domain is decomposed into eight sub-domains as defined in the PRUDENCE project (Christensen et al. 2007) and representing homogenous climatic settings (Fig. 1). For illustrating elevation dependencies, the RCM grid cells in each sub-domain are pooled according to their mean grid cell orography into 100 m-elevation bins (0–100 m, 100–200 m, etc.). Of the eight sub-domains, only the Alps (AL) have a considerable fraction of their total land area located above 2000 m (see ESM Part A). Further regions with a substantial contribution of high-elevation grid cells above 1000 m are the Iberian Peninsula (IP) and the Mediterranean (MD).[2] For testing the statistical significance of changes in mean values we employ the two-sided Wilcoxon-Mann-Whitney rank-sum test (Wilks 2006) at a 99% confidence level. This includes the assessment of significant temperature or precipitation changes at grid cell or elevation band level as well as the test whether the mean climate change signal in a given elevation interval (mean change of all grid cells in that interval) is significantly different from the sub-domain mean change (mean change of all grid cells in the entire sub-domain).

[2] As a general rule and unless stated otherwise, we will apply the terms *low*, *medium* and *high elevation* in a relative sense, i.e., with respect to the elevation range covered by each individual sub-domain. For instance, *high elevations* in sub-domain AL will refer to a different elevation range (> about 1500 m) than *high elevations* in sub-domain BI (> about 400 m).

4 Results

4.1 Validation of RCM elevation gradients

Figures 2 and 3 present a comparison of the elevation dependency of mean annual 2 m temperature and mean annual precipitation in CCLM-ERA40 and CCLM-HadCM3 against E-OBS for the period 1961–2000. Both experiments approximately capture the observed temperature decrease with elevation (Fig. 2). Also deviations from the linear fit are well represented. Mean lapse rates, however, are overestimated in all sub-domains. This overestimation could be connected to a bias of the environmental lapse rate, which is not assessed in detail here. Largest deviations from the observed lapse rate of more than 0.1°C $(100\ \mathrm{m})^{-1}$ occur in sub-regions AL, FR and EA. As a result, the model bias in these regions is not constant with elevation but becomes strongly negative at elevations above 1000 m (FR: 500 m) compared to a slight positive bias in lower-elevation grid cells. In sub-domain AL the two reference datasets E-OBS and ZAMG closely agree with each other, both with respect to the general temperature level and the temperature lapse rate. Obviously, the lower station density in E-OBS does not hinder an accurate assessment of mean annual temperature in the Alpine region and its elevation dependency. In the north-western sub-domains BI, ME and SC the temperatures in CCLM-HadCM3 are lower than in CCLM-ERA40 over the entire elevation range. This systematic difference is probably inherited from the driving global model. Along the north-western boundary of the RCM domain, which is the predominant inflow boundary, HadCM3 shows a pronounced cold bias in the annual mean compared to ERA40 (not shown). Interestingly, the lapse rates in CCLM-ERA40 and CCLM-HadCM3 are very close to each other despite the cooler conditions in CCLM-HadCM3.

The elevation dependency of annual precipitation is far more complex and the linear fit only provides a rough estimate of its characteristics (Fig. 3). CCLM shows a pronounced wet bias at elevations below 1000 m in most regions. The general increase of precipitation with elevation is approximately captured by both model experiments up to elevations of about 1000 to 1500 m. The most striking discrepancy between CCLM and E-OBS is the decrease of the simulated precipitation sums at high elevations of individual sub-domains, leading to pronounced dry biases (e.g., AL, EA, IP). In sub-domain AL, simulated precipitation is in close agreement with the high-resolution dataset S2001 at elevations below 1000 m while, again, precipitation is underestimated at high altitudes. At elevations above 500 m, pronounced differences exist between the two references E-OBS and S2001. These differences are of the same order of magnitude as the model bias. They highlight the potential influence of inaccuracies in the reference data on the model evaluation. Still, the dry bias of CCLM at elevations above 2000 m in the Alps is a robust feature found for both reference datasets. A seasonal analysis (not shown) reveals that in the affected regions the high-elevation dry bias typically occurs throughout the entire year and is not restricted to individual seasons. Presumably, the wet bias at low elevations and the dry bias at high elevations of individual sub-domains are connected to each other. In case of topographically lifted air masses, excessive precipitation at low altitudes upstream could cause a gradual drying of the air and prevent the formation of precipitation later on at higher altitudes. In addition, the model bias is likely affected by the neglect of the horizontal transport of falling hydrometeors in the current model version (see Verbunt et al. 2007). It is worth noting that the findings presented above are influenced by the fact that both E-OBS and S2001 provide precipitation sums that are not corrected for the systematic undercatch of rain gauges (e.g., Adam and Lettenmaier 2003). In a relative sense, this undercatch can be expected to be

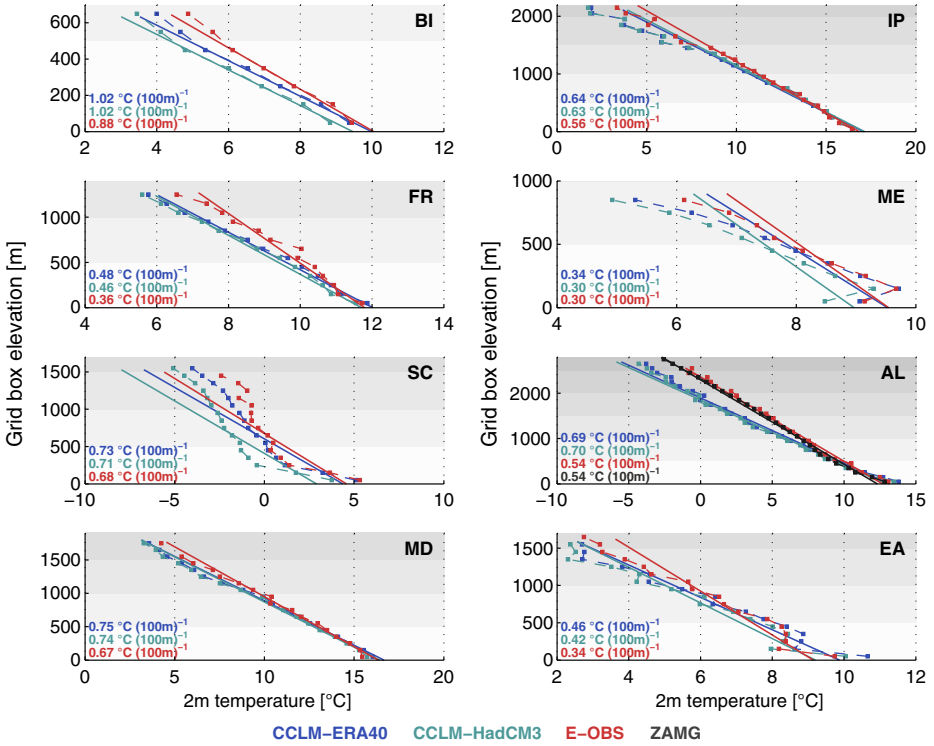

Fig. 2 Elevation dependency of mean annual 2 m temperature in CCLM-ERA40 (*blue*), CCLM-HadCM3 (*green*) and E-OBS (*red*) for the period 1961–2000 and for the eight sub-domains. For sub-domain AL the high-resolution ZAMG dataset, based on the period 1961–1990, is shown in addition (*black*). *Dashed lines*: mean 2 m temperature for each 100 m elevation interval; *solid lines*: linear regression (least squares fit) through all individual grid cells; numbers in the lower left corner of each panel: 2 m temperature lapse rates (based on linear regression). The *gray background shading* indicates 500 m elevation bands. The same shading is used for all sub-domains to allow for a better inter-comparison

larger at high elevations due to a larger fraction of snowfall and stronger winds. Correcting for the precipitation undercatch would decrease the wet bias of CCLM at low elevations but would amplify the model's dry bias in high regions (which, still, could be caused by a too fast drying of topographically lifted air masses as explained above). Similarly to 2 m temperature, there is a good agreement between the elevation dependency of mean annual precipitation in CCLM-ERA40 and CCLM-HadCM3.

In summary, the simulated and observed elevation gradients approximately match each other. The agreement is better for temperature than for precipitation. It provides basic confidence into the ability of CCLM to accurately capture the governing processes. This is supported by the validation on a monthly time scale (see ESM Part B): in all sub-domains CCLM approximately reproduces the observed annual cycle of the elevation dependency of both parameters. Furthermore, the model is able to reproduce the observed year-to-year variability of elevation gradients in most cases (ESM Part C). This provides further confidence into the ability of the model to accurately represent also the response of elevation gradients to climate change.

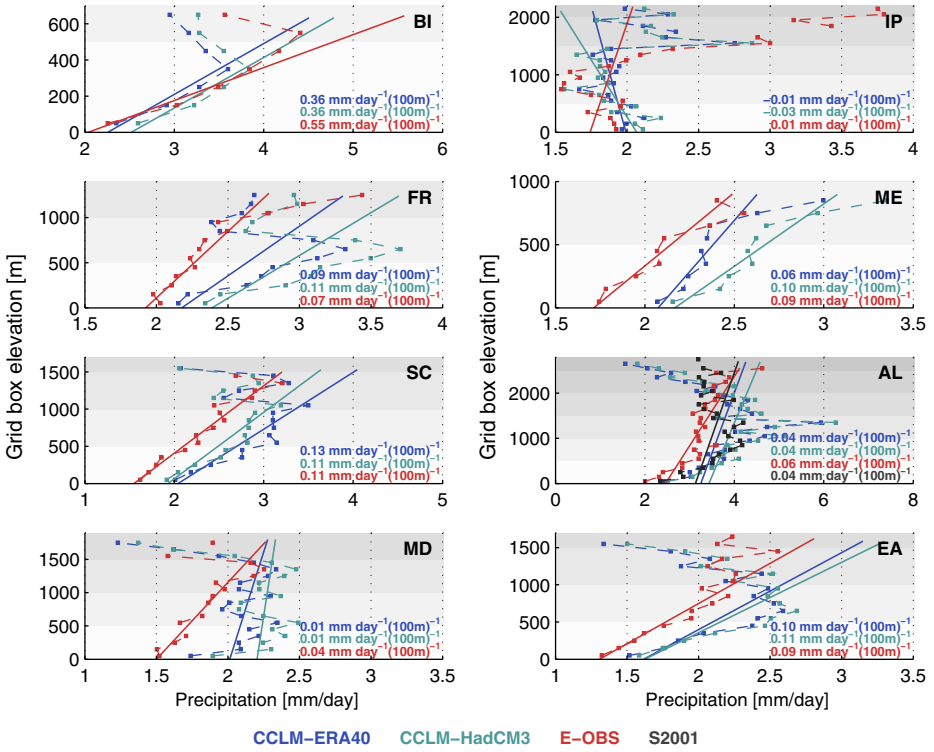

Fig. 3 As Fig. 2 but for mean annual precipitation. For sub-domain AL the high-resolution observational dataset S2001, based on the period 1971–1990, is shown in addition (*black*). Numbers in the lower right corner of each panel: precipitation change with altitude (based on linear regression)

4.2 Temperature climate change signal at 2 m

4.2.1 European scale

Figure 4 provides a European-scale picture of the simulated change of mean winter and summer 2 m temperature until the end of the 21st century (CCLM-HadCM3). In both seasons the temperature change exhibits a pronounced spatial variability but is positive and significant throughout Europe. In winter, the largest warming of more than 5°C occurs in North-Eastern Europe while temperature increases of less than 3°C are simulated over the Iberian Peninsula, the British Islands and Western France. In summer a different pattern emerges with Southern Europe experiencing the largest temperature increase of more than 4°C and only a moderate warming in the northern parts. Qualitatively, these seasonal warming patterns agree with those simulated by the driving GCM HadCM3, but pronounced differences exist on a regional scale especially concerning the amplitude of the warming (ESM Part D). The basic warming patterns also agree with those found in previous studies (e.g., Christensen and Christensen 2007). The equal-elevation contour lines in Fig. 4 allow a first comparison of warming rates between high and low altitudes on a qualitative basis. In many regions, the simulated warming seems to intensify with elevation, though only marginally in DJF compared to JJA (Pyrenees in DJF and JJA, Alps in DJF and JJA, Carpathians in JJA, Scandinavian Alps in JJA, Iberian Meseta in JJA). The

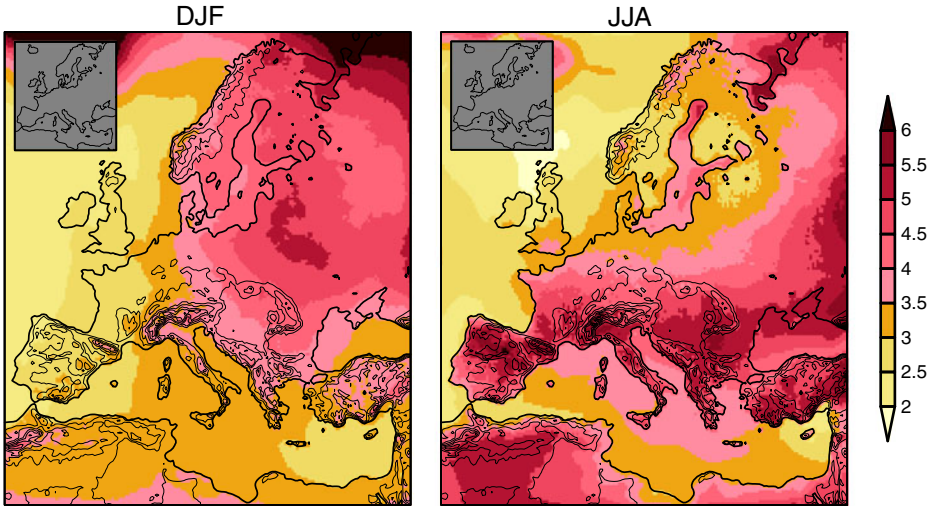

Fig. 4 Simulated change of mean winter (DJF, *left*) and summer (JJA, *right*) 2 m temperature between 1961–1990 and 2070–2099 [°C]. The contour lines represent the model topography at 400 m intervals. The gray color in the maps in the upper-left corner indicates regions where the seasonal temperature change is significant at the 99% confidence level

warming over ocean surfaces is typically less pronounced than over adjacent land grid cells (except for the Baltic Sea in summer).

4.2.2 Elevation dependency in sub-domains

The comparatively strong warming at high elevations is confirmed by Fig. 5 which shows the mean seasonal 2 m temperature change as a function of elevation. In all sub-domains and at all elevations the climate change signal is positive and significant (black markers). Warming rates can vary considerably with elevation and individual elevation bands can show temperature changes that are significantly different from the regional mean change (open circles). Only elevations that experience a similar warming compared to the sub-domain mean (e.g., medium elevations in IP in winter) or that show a different warming compared to the sub-domain mean but only contain very few grid cells (e.g., high elevations in AL in summer) fail to pass the significance test. In most regions, the warming intensifies with elevation and can often be approximated by a linear function of altitude. Exceptions are BI in summer, EA in winter and SC in winter and spring where low-elevation regions show the largest warming. On a seasonal basis, the strongest variations of the 2 m temperature change with elevation occur in summer while autumn shows rather weak gradients (IP, FR, ME, AL, MD, EA). A special pattern emerges in the Alps in summer when both high- and low-elevation regions (>2000 m and <500 m, respectively) experience a strong temperature increase while the warming is less pronounced at medium elevations (500–1500 m). A likely explanation is the spatial extent of sub-region AL which includes the low-lying Po valley in its southern parts. In spring, the largest warming in sub-domain AL occurs at medium elevations between 1500 and 2000 m and is significantly different from the regional mean warming. This is consistent with Swiss temperature trends observed during the second half of the 20th century and points to the influence of snow cover changes close to the zero-degree

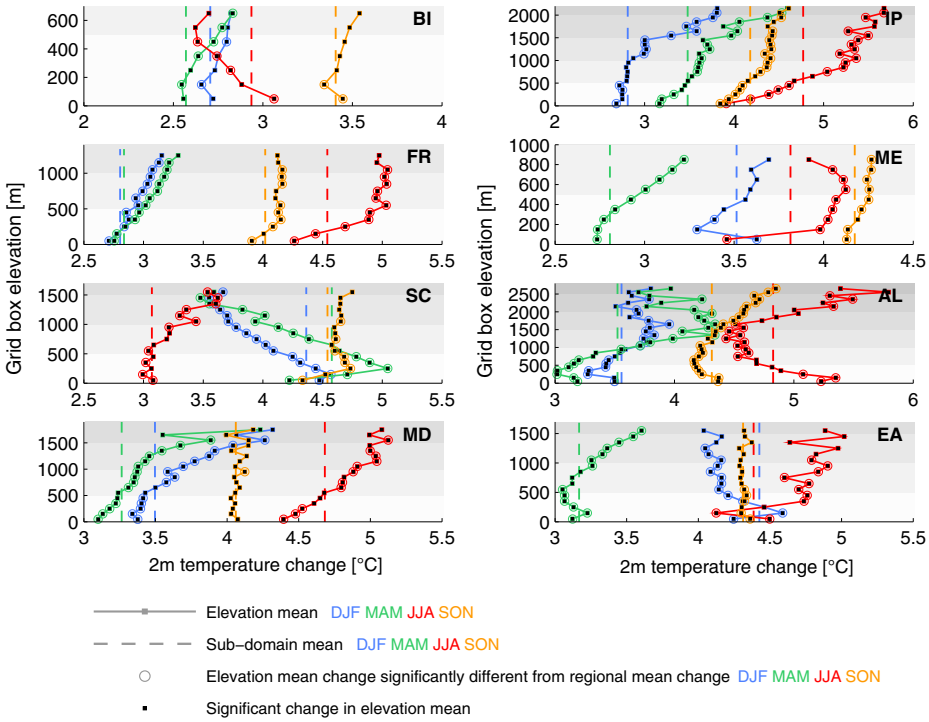

Fig. 5 Simulated change of mean seasonal 2 m temperature between 1961–1990 and 2070–2099 [°C] in each 100 m elevation band for all seasons and sub-domains. Black squares indicate a significant elevation mean change between the control and the scenario period. Circles highlight an elevation mean change which is significantly different from the sub-domain mean change. The gray background shading indicates 500 m elevation bands. The same shading is used for all sub-domains to allow for a better inter-comparison

isotherm (Ceppi et al. 2010; see also Chapter 3.4.1). The described pattern of larger warming rates at high elevations results in a decrease of the near-surface temperature lapse rate in most sub-domains and in most seasons (less pronounced temperature decrease with elevation). Typically, this effect is largest in summer with lapse rates decreasing by more than 0.1°C (100 m)$^{-1}$ in sub-domains IP, FR and ME (ESM Part E).

4.3 Precipitation climate change signal

4.3.1 European scale

As for temperature, a pronounced spatial variability of the precipitation change over Europe is simulated (Fig. 6). On a regional scale, it can in some cases be connected to the grid box elevation. While most of Europe experiences a precipitation increase in winter (which is significant only in the north-eastern parts), high-elevation regions in the Alps and the Pyrenees show a slight decrease of winter precipitation. In contrast, high elevations along the eastern rim of the Scandinavian Alps, in the Carpathians and in the Balkans experience an above-average increase of precipitation. Besides an elevation effect, winter precipitation changes are obviously also influenced by the relative setting of

a grid cell in the regional topographic context. For instance, winter precipitation increases along the southern slopes of the Alps while it decreases along the northern rim. A similar dependency of precipitation changes on the slope direction is evident for the Scandinavian Alps, the Pyrenees, and the Balkan Mountains, which indicates an influence of regional circulation changes on the precipitation change signal. In summer, a pronounced and significant drying is simulated for the central and southern parts of Europe with summer precipitation decreasing by more than 60% over most parts of the Iberian Peninsula. This precipitation change pattern is consistent with previous studies (e.g., Christensen and Christensen 2007). Again, elevation dependencies of the precipitation change appear on a regional scale. A slight increase of precipitation occurs along the main Alpine ridge compared to a drying signal in the surrounding areas. Similarly, the percentage increase of summer precipitation is larger along the main ridge of the Scandinavian Alps compared to low-elevation areas. Most of these findings also apply to the absolute changes of precipitation sums (not shown). As for temperature, the seasonal precipitation change patterns simulated by CCLM agree qualitatively with those of the driving GCM HadCM3, but can vary considerably on a regional level (see ESM Part D).

4.3.2 Elevation dependency in sub-domains

Figure 7 provides a clearer picture of the elevation gradient of seasonal precipitation changes. Except for SC and parts of BI and IP, the pattern of summer-drying and winter-wettening is reflected in all regions and throughout the entire elevation range (red and blue lines compared to the zero change). The spring and autumn climate change signals are typically located in-between the winter and summer signals and are of smaller magnitude (e.g., ME, AL, MD, EA). The significance of precipitation changes strongly depends on the season and only little on elevation. The summer drying signal is significant in most sub-regions while significant changes in winter, spring and autumn precipitation are obtained only in a few areas. In many regions, the elevation dependency of relative precipitation changes is considerable but only a few consistent signals valid over a range of different sub-

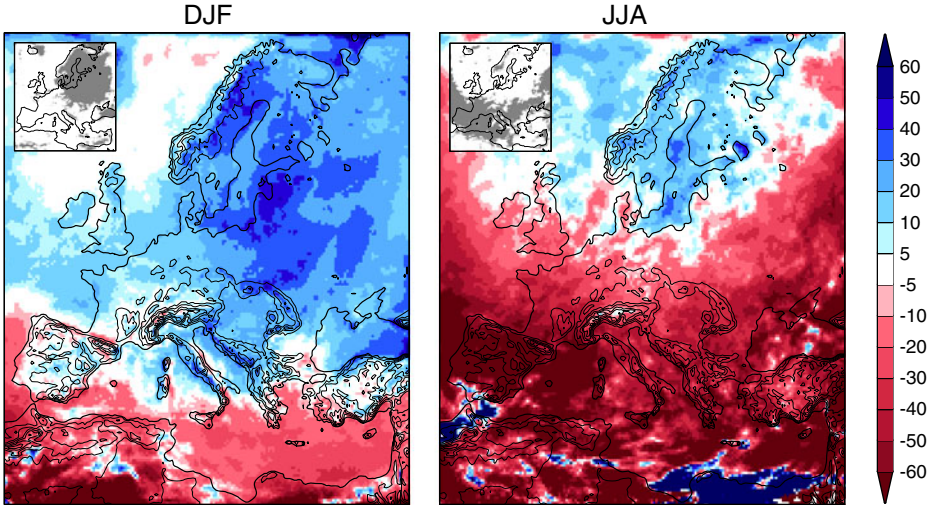

Fig. 6 As Fig. 4 but for mean seasonal precipitation [%]

domains emerge. In the mountainous regions IP, SC, AL and MD the relative decrease of mean summer precipitation becomes less pronounced with elevation and can differ significantly from the regional mean change in the uppermost grid cells (open circles). The opposite is the case for sub-regions FR and EA where the summer drying becomes more intense when moving from low to high elevations. The winter wettening signal typically increases with elevation, but there are exceptions to this as well (FR, SC, AL). Hence, compared to temperature the simulated elevation dependency of relative precipitation changes is subject to a pronounced variability in space (sub-domain) and time (season), which reflects the complexity of processes involved in the formation of precipitation.

4.4 Climate change signals of additional parameters

Changes in 2 m temperature and precipitation are key parameters in climate impact studies, but climate change is not restricted to these quantities. The output of physically based regional climate models offers the possibility to analyze a large number of further parameters at the scales resolved by the model. Many of these parameters are of high relevance for impact research, such as future changes in snow cover characteristics or insolation. Furthermore, within the complex climate system their changes could be connected to changes in temperature and precipitation and their analysis could give insight into possible mechanisms responsible for the findings presented in the previous chapters.

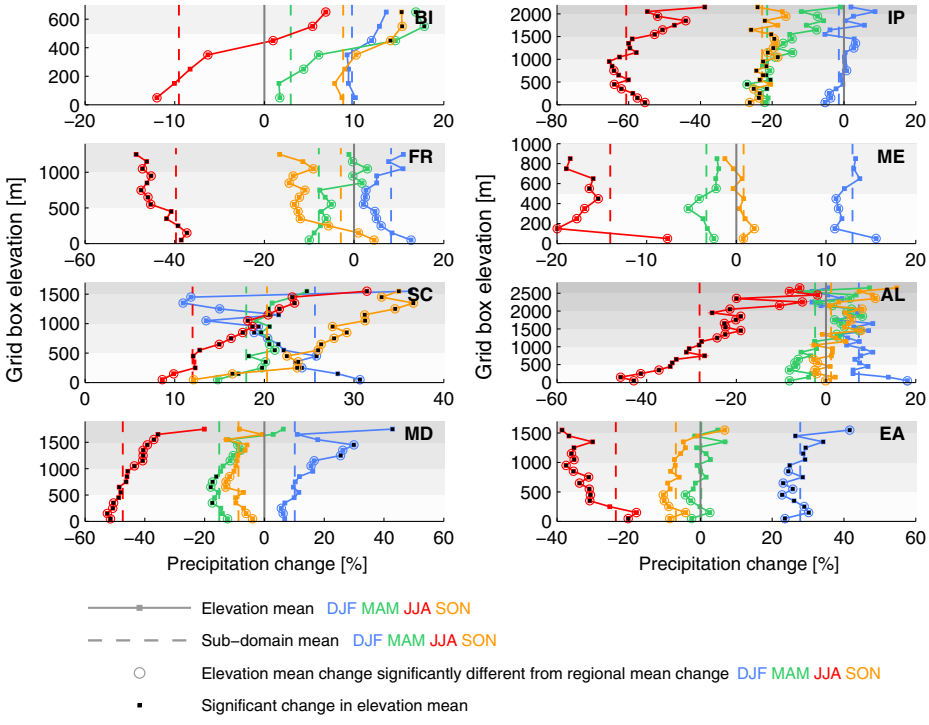

Fig. 7 As Fig. 5 but for mean seasonal precipitation [%]

4.4.1 Snow cover

As a result of the higher temperature level and despite the simulated increase of winter precipitation, seasonal snowfall amounts decrease in all sub-domains and at almost all elevations (not shown). In addition, snow that has settled on the ground is subject to a more rapid melt due to higher temperatures. In combination, the decreasing snowfall amounts and the faster snow melt on the ground lead to a strong reduction of the number of snow days (defined as days on which the simulated grid cell mean snow depth exceeds a threshold of 0.003 m w.e.) at all elevations which is significant in most regions (Fig. 8). Even high-elevation Alpine grid cells located above 2000 m experience a considerable shortening of the snow season and low-elevation areas in all sub-domains are facing losses by often more than 80%. In general, the percentage decrease of the number of snow days (dashed lines) becomes smaller when moving from low to high elevations while the absolute decrease (solid lines) enlarges. Prominent exceptions are sub-regions SC and AL in winter and spring, where the maximum absolute loss is simulated at low (SC, <500 m) or medium (AL, 1500–2000 m) elevations. Obviously, the high amounts of winter snowfall in the control climate combined with the simulated increase of wintertime precipitation help to sustain an extended snow season at high-elevation grid cells in these two sub-domains.

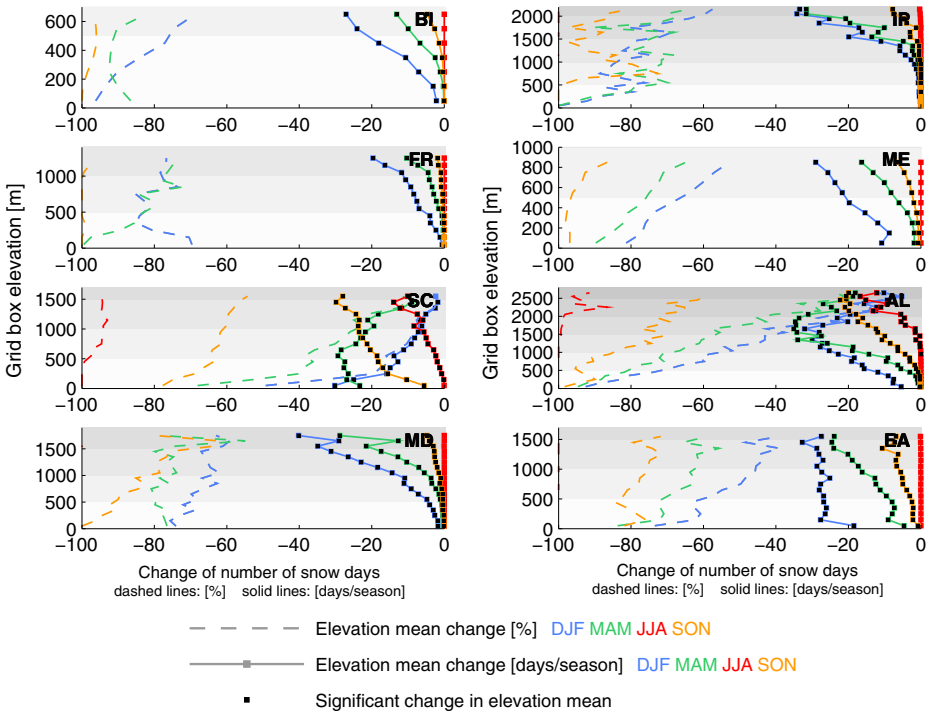

Fig. 8 Simulated change of the mean number of snow days between 1961–1990 and 2070–2099 in each 100 m elevation band for all seasons and all sub-domains. *Dashed lines*: relative change [%], *solid lines*: absolute change [days/season]. The same x-axis scale is used for both relative and absolute changes. *Black squares* indicate a significant change at the respective elevation. The *gray background shading* indicates 500 m elevation bands. The same shading is used for all sub-domains to allow for a better inter-comparison

4.4.2 Surface albedo

Within the CCLM land surface parameterization scheme, the grid cell surface albedo is internally computed as a function of the soil type, the fractional plant cover, soil moisture and snow cover. Consequently, the simulated decrease of snow cover is reflected in changes of the surface albedo (Fig. 9). In all sub-domains and at all elevations, the albedo change closely follows the change in the absolute number of snow days (solid lines in Fig. 8) Maximum albedo reductions of around 0.2 occur at medium to high elevations in sub-domains AL (1500–2000 m) and MD (>1500 m) in winter and spring.

4.4.3 Surface net shortwave radiation

The described changes of the surface albedo alter the amount of solar radiation absorbed by the surface and should therefore be reflected in changes of the shortwave radiation budget. The latter is furthermore influenced by changes of incoming solar radiation which, in turn, strongly depends on cloud cover. An analysis of the simulated cloud cover changes (ESM Part F) reveals that in most sub-regions, strong and significant decreases of cloud cover occur in summer and autumn while changes of winter and spring cloud cover are rather small and show only little elevation dependency. Except for sub-domains BI and SC, the summertime cloud cover reduction is connected to an increase of incoming solar radiation especially at high elevations

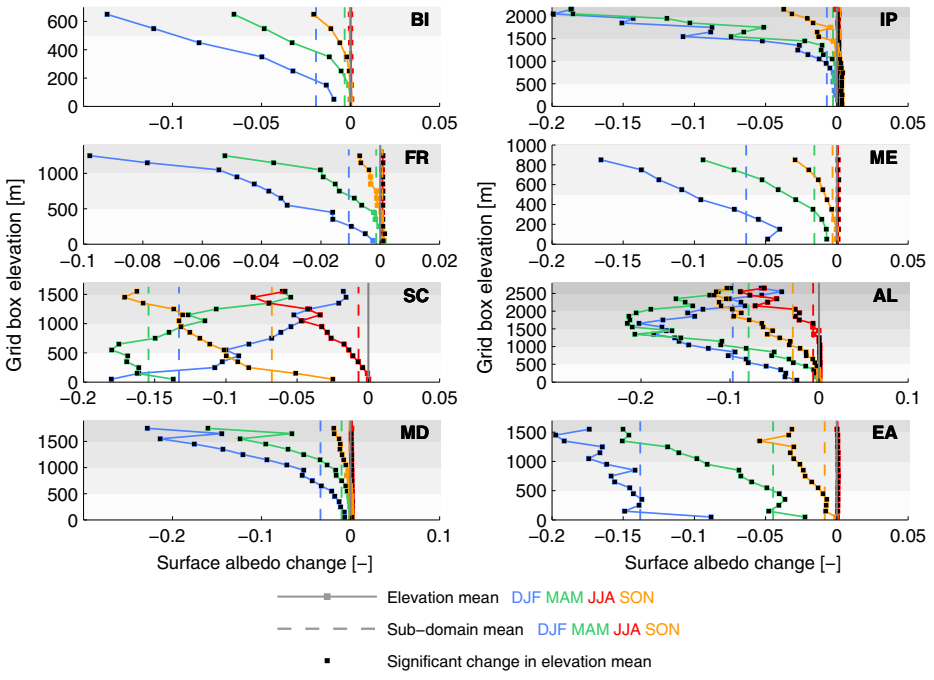

Fig. 9 Simulated change of mean seasonal surface albedo between 1961–1990 and 2070–2099 [−] in each 100 m elevation band for all seasons and sub-domains. *Black squares* indicate a significant change at the respective elevation. The *gray background shading* indicates 500 m elevation bands. The same shading is used for all sub-domains to allow for a better inter-comparison

(ESM Part F) . Even in the absence of surface albedo changes this effect alone leads to an increase of net surface solar radiation (Fig. 10; e.g., sub-domains IP, FR, ME and MD). In winter and spring, on the other hand, surface albedo changes obviously dominate the variation of net shortwave radiation changes with elevation and can even reverse elevation dependencies introduced by changes in surface incoming solar radiation (i.e., dependencies introduced before the surface albedo acts on the surface radiation budget). This becomes very obvious in sub-domain AL where the elevation range showing the maximum increase of MAM net shortwave radiation by up to 28 Wm^{-2} corresponds exactly those elevations that experience the strongest decrease in surface albedo. In the same elevation range, surface incoming solar radiation actually decreases by a similar magnitude (see ESM Part F).

4.4.4 Snow cover change vs. 2 m temperature change

The previous findings suggest a strong influence of snow cover changes on winter and spring temperature changes via changes in surface albedo and net shortwave radiation (snow-albedo feedback). This impression is confirmed by Fig. 11 which shows the relation between the regional anomaly of changes in the number of snow days and the 2 m temperature change anomaly (anomalies denote the mean change in the individual elevation bands minus the sub-domain mean change). In most regions, a clear relation between both quantities exists in winter and spring. Correlation coefficients are often lower than −0.9, indicating a clear negative relation between the deviation of the temperature change in a certain elevation band from the regional mean and the snow day change anomaly. Simply

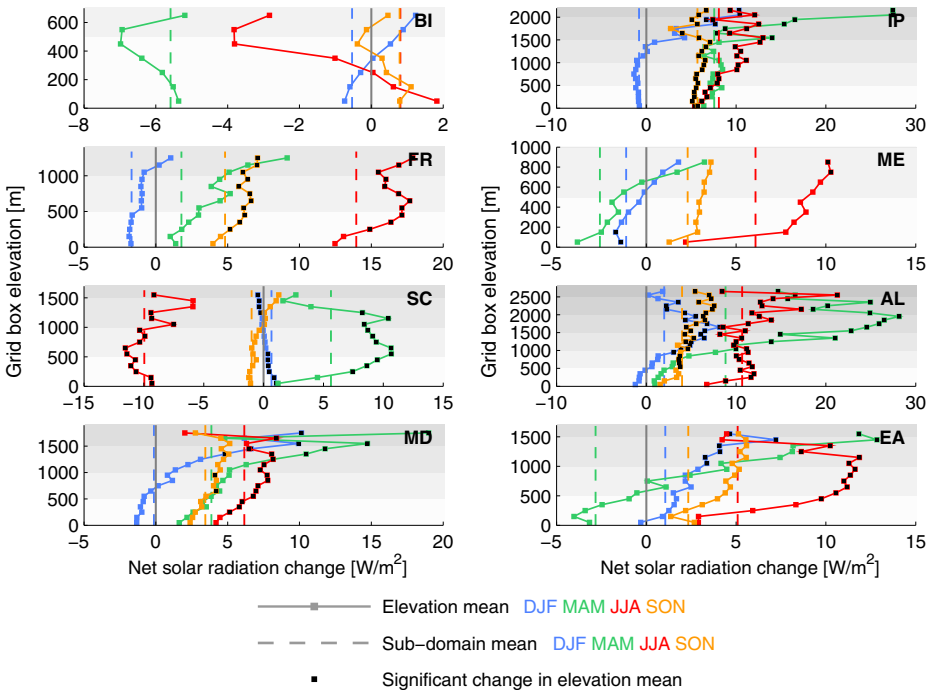

Fig. 10 As Fig. 9 but for net surface solar radiation [W/m^2]

speaking, an above-average temperature increase is associated with a comparatively large reduction in the number of snow days, and vice versa. In some regions also summer (SC, AL) and autumn (BI, ME, SC, AL) show strong correlations. Note that the strong relation between winter and spring snow cover changes and temperature changes as presented in Fig. 11 is not necessarily a consequence of the snow-albedo feedback. It could also contain large-scale warming signals to which snow cover is reacting passively.

4.5 Temporal evolution of 2 m temperature changes

So far, our analysis of climate change signals focused on the period 2070–2099. The transient character of the CCLM-HadCM3 experiment offers the possibility to also investigate the temporal evolution of climatic changes and their elevation dependency during the entire simulation period 1950–2099. Adopting the analysis of Fyfe and Flato (1999) and focusing on mean annual 2 m temperature, we present in Fig. 12 the 30-year running mean climate change signals with respect to 1961–1990 for all elevation bands and all sub-domains. In order to assess the suitability of temperature changes at distinct elevations as early indicators of larger-scale warming, we also denote the point in time at which the temperature change at a particular elevation becomes significant (99% level) and remains significant for the rest of the simulation (white lines). In most parts of Europe, elevation dependencies of the heating rate become apparent only after about 2020. Before that, the 2 m temperature change is rather homogenous. This is very probably connected to the fact that also snow cover changes are homogenous before 2020 and show only a week dependency on elevation (not shown). Pronounced elevation gradients of the temperature change arise up from 2040 with most regions experiencing a stronger annual mean warming at high elevations. However, the stronger heating in these regions does not imply an earlier significance of the temperature change. The time at which warming signals become detectable depends only little on elevation and is reached around the year 2000 in all sub-domains and at all elevations, i.e., before elevation dependencies of the warming signal

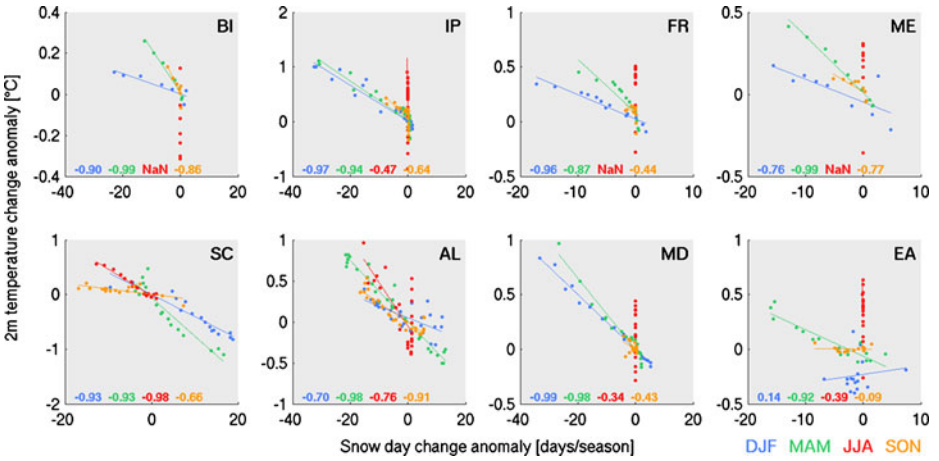

Fig. 11 Snow day change anomaly versus 2 m temperature change anomaly (2070–2099 w.r.t. 1961–1990) for all seasons and sub-domains. Each marker represents one 100 m elevation band and shows the anomalies of changes in that elevation with respect to the sub-domain mean change. The numbers in the lower row of each panel denote the seasonal correlation coefficients (NaN: no correlation coefficient could be computed)

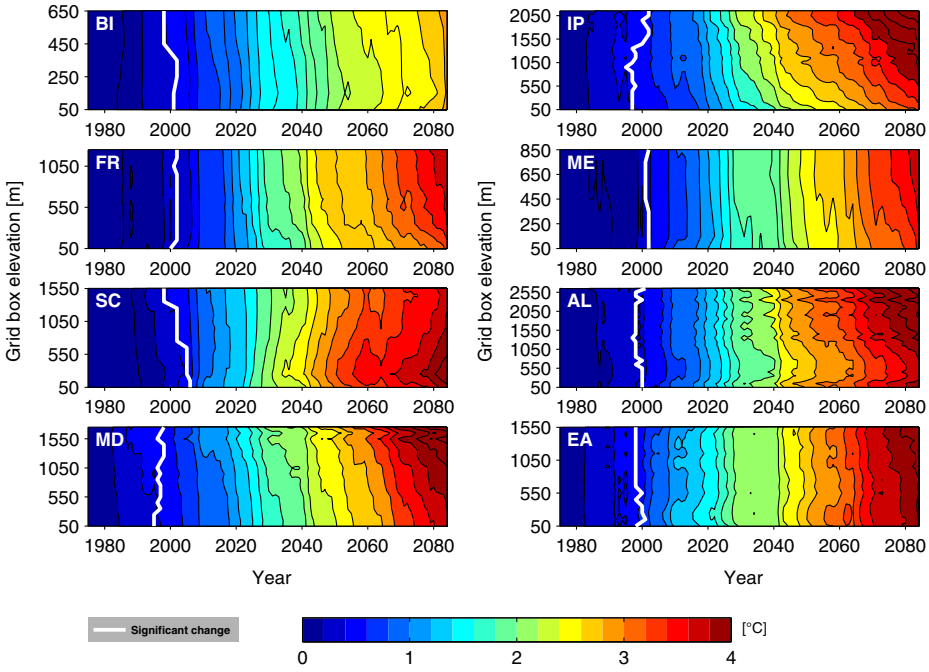

Fig. 12 Temporal evolution of the mean annual 2 m temperature change (30-year centered running mean w.r. t. 1961–1990) as a function of elevation and for all sub-domains. The *white lines* denote the year, in which temperature changes at a certain elevation become significant (99% level) and remain significant for the rest of the simulation

come into play. These findings basically also apply to seasonal temperature changes (not shown). They are in line with the analysis of Fyfe and Flato (1999) for the Rocky Mountains who also found no early detection potential associated with the anomalous high-elevation warming.

4.6 Changes of tropospheric air temperature

In addition to land surface processes occurring on regional scales, also large-scale changes of the environmental lapse rate can have an influence on the elevation dependency of the near-surface temperature change. To explore this aspect in more detail, we compare the elevation profiles of the simulated changes in 2 m temperature and the simulated changes of the free-tropospheric air temperature (given by the temperature change at the mean height of the 1000, 925, 850, 700, 500, and 300 hPa pressure levels in each sub-domain). This analysis can only provide a broad and qualitative idea on the potential influence of environmental lapse rate changes on near-surface conditions, as a separation of the different influences is not possible in our model setup. As can be seen from Fig. 13, the simulated changes of the tropospheric air temperature show a clear elevation dependency. In most cases largest warming rates occur in the middle to upper troposphere resulting in an overall decrease of the environmental lapse rate. This is consistent with theoretical considerations and global-scale modeling studies (see introductory section). Part of the elevation signal of the near-surface temperature change might therefore be caused by larger-scale changes of

the free-tropospheric air temperature. However, in many cases the elevation dependency of 2 m temperature changes in the elevation range covered by the model topography (gray-shaded area) is more pronounced and much more variable than for the tropospheric air temperature. This indicates that large-scale processes in the free troposphere cannot fully explain near-surface temperature changes and that, very probably, local and regional-scale processes involving the land surface have a strong influence. A prominent exception is the winter and spring temperature change in sub-domain SC. Here, the decreasing warming signal with elevation in the lower troposphere is reflected both by the 2 m temperature and the tropospheric air temperature which indicates a strong coupling between both quantities in the Scandinavian region and, eventually, a stronger influence of tropospheric temperature changes.

4.7 Refined analysis removing large-scale components

The sub-domain-based analysis presented above does not exclusively reveal elevation signals but can include imprints of large-scale horizontal variability. In case that the large-scale gradient of a near-surface parameter (e.g., North–South pattern of warming) coincides with a topographic gradient, this effect can mask "true" elevation effects (i.e., elevation dependencies of near-surface climate change that are indeed governed by the topographic

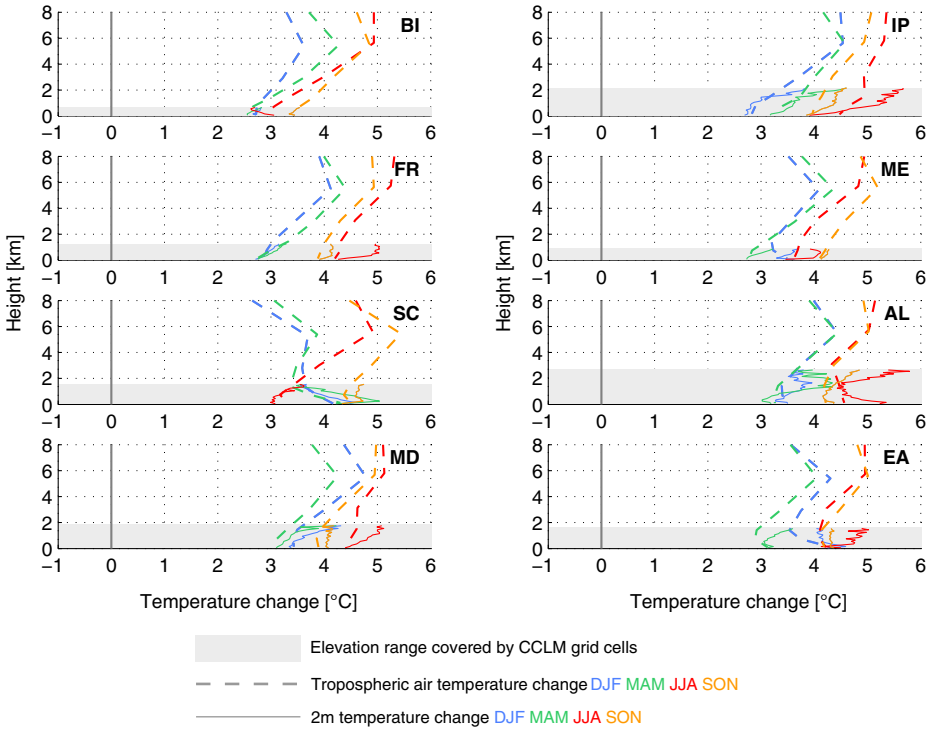

Fig. 13 Comparison of free-tropospheric and 2 m temperature changes between 1961–1990 and 2070–2099 [°C] for all seasons and all sub-domains up to a height of 8 km. *Bold dashed lines* indicate changes of the tropospheric air temperature (based on the temperature at 1000, 925, 850, 700, 500, and 300 hPa), *thin lines* denote changes of the near-surface air temperature in 100 m grid cell elevation bands (see also Fig. 5). The gray-shaded area indicates the elevation range covered by the RCM topography

height). Especially the large sub-domains SC, EA and MD can be expected to also sample the continental-scale West-East and North–South gradients of surface climate change (see Figs. 4 and 6). Further candidates are the high-elevation summer warming in sub-domains EA and ME.

In order to address this point we here employ a heuristic method to reduce the influence of large-scale components onto the near-surface climate change signal. The procedure is explained in detail in the ESM Part G and, for the example of 2 m temperature, consists of deriving the large-scale component ΔT^{ls} of the temperature change by applying a simple spatial filter onto the pattern of the grid-cell-based 2 m temperature change ΔT. The spatial pattern of ΔT^{ls} contains only little regional variability (see Figure ESM 10), which justifies the applicability of our heuristic method. In a second step, ΔT^{ls} is removed from ΔT for each grid cell, yielding the temperature change ΔT^* without the influence of large-scale components, i.e., containing mostly regional-scale variability. The same procedure is applied for precipitation changes.

Figure 14 presents the analysis of elevation dependencies of ΔT^* in the individual sub-domains in addition to those of ΔT. In most cases removing the large-scale contribution has only little influence on the elevation dependency of the 2 m temperature change, indicating that regional-scale processes play a dominant role. But there are some exceptions to this. In sub-domain BI, summer ΔT^* is almost constant with elevation while ΔT shows largest increases at low elevations and is obviously strongly controlled by the continental-scale pattern. Also the comparatively large summer warming at high elevations in sub-domains FR, MD, ME and EA mostly has to be attributed to large-scale patterns. Removing the large-scale signal in sub-domain EA even yields a decrease of autumn warming with elevation. The prominent summer warming at elevations below 500 m in the European Alps is slightly reduced but still present. Obviously, the strong summer temperature increase in the Po Valley can only partly be linked to large-scale processes. It might be triggered by regional land-atmosphere feedback processes involving soil moisture which, however, has not been assessed in detail. In case of precipitation, removing the large-scale component has only little influence on the elevation dependency of the climate change signal (not shown). A clear effect can only be established for the decrease of summer precipitation in sub-domains FR, EA and ME. In these cases, removing the large-scale signal results in a less strong precipitation decrease at high elevations compared to low-lying grid cells, yielding similar precipitation decreases at all elevations.

5 Discussion

The results presented in the previous chapter indicate that (i) CCLM is able to approximately reproduce observed altitudinal variations of 2 m temperature and precipitation and that (ii) the simulated 21st century climate change is subject to a pronounced elevation dependency in many regions. Our analysis of possible reasons for this dependency focuses on several factors, among these vertical gradients in the free-tropospheric warming and regional-scale processes as simulated by the RCM.

A robust finding is that over most parts of Europe and in most seasons, near-surface warming significantly increases with elevation. This is consistent with the free-atmospheric height dependency of warming but cannot be fully explained by the latter. In winter and spring, the strong high-elevation warming is closely connected to the decrease in the number of snow days. Our analysis only reveals the existence of such a relation but not the direction of a possible cause-effect mechanism. The question is whether the high-elevation

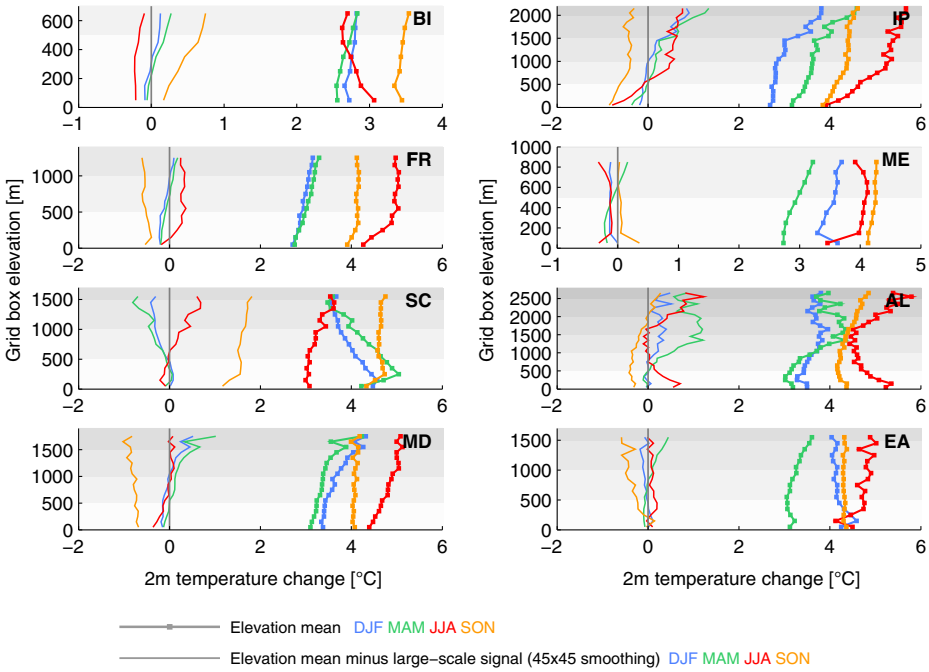

Fig. 14 Simulated change of mean seasonal 2 m temperature between 1961–1990 and 2070–2099 [°C] in each 100 m elevation band for all seasons and all sub-domains. *Bold marked lines* indicate the total change (ΔT, compare to Fig. 5), *thin lines* denote the deviation ΔT^* of the total temperature change at the respective elevation from the large-scale signal ΔT^{ls} (obtained by a 45×45 grid cell smoothing). The gray background shading indicates 500 m elevation bands. The same shading is used for all sub-domains to allow for a better inter-comparison

changes in snow cover are simply a result of anomalously large warming rates (governed for instance by large-scale processes) or whether the snow-albedo feedback mechanism is acting, amplifying the warming in areas of strong snow cover reduction. Our results favor the second option since the relation between the 2 m temperature change anomaly at a certain elevation and the absolute or percentage anomaly of changes in snow water equivalent (SWE; not shown) is typically weaker than for the changes of the number of snow days. If no feedback mechanisms were acting (higher temperatures determining snow cover changes with no feedback on temperature), changes in SWE should have a stronger relation to temperature changes as they are a direct consequence of an elevated temperature level with the number of snow days (SWE above a certain threshold) being only indirectly affected. Furthermore, a clear physical mechanism can be established with decreasing snow cover causing a decay of the surface albedo and an increase of net solar radiation, resulting in an energy gain of the land surface. A pre-requisite for an appropriate representation of future influences of the snow-albedo feedback in CCLM is a proper representation of snow cover characteristics. Indeed, CCLM is able to approximately reproduce the spatial and temporal characteristics of contemporary European snow cover (see ESM Part H).

In addition to winter and spring, also parts of the elevation gradients of summer and autumn temperature change can be explained by the snow-albedo feedback in sub-domains AL and SC. This is not the case for summer temperature changes in other sub-domains, e.g., for the anomalous high-elevation summer warming in

Southern Europe (IP, FR, MD, EA). For FR, MD and EA part of this signal can be attributed to the geographical extent of the domains and the large-scale component of climate change. For sub-domains IP and MD a further point is the proximity of low-elevation regions to the coastline of the Mediterranean Sea and the Atlantic Ocean, both of which show a considerably smaller increase of near-surface air temperature than land areas (see Fig. 4). Especially during summer, the low-elevation warming closely follows the warming of sea-surface temperatures that control coastal temperatures (see ESM Part I). In sub-region IP, a further factor contributing to high-elevation summer warming is a considerable decrease of soil moisture leading to an increased flux of sensible heat towards the atmosphere at the expense of surface evaporation, amplifying the large-scale warming signal at high altitudes.

As for 2 m temperature, the analysis of precipitation changes does not only reveal elevation signals but also includes continental-scale spatial variability. This is especially true for the summer season with its pronounced North–South pattern of precipitation change. The latter is reflected by the strong decrease of precipitation at high elevations in sub-domains FR, EA and ME. All other regions experience a rather modest summer drying at high elevations while the drying signal becomes more pronounced at low altitudes. A detailed analysis (not shown) reveals that the elevation dependency of the precipitation change is mainly controlled by changes of grid-scale precipitation (resolved scale), while changes of convective precipitation (subgrid-scale, simulated by CCLM's convective parameterization scheme) often play a minor role. Exceptions to this are elevation gradients of summer precipitation change in sub-domains IP and AL which seem to be much more determined by changes in the convective precipitation amount.

Relating to previous studies, our results confirm the findings of Giorgi et al. (1997) for the Alpine region as far as temperature changes are concerned. In many regions, changes in surface snow cover and the snow-albedo feedback can be identified as driving factors for the amplification of seasonal warming rates at high elevations. However, an early detection potential of the high-elevation warming for large-scale temperature changes is not found. This is in line with the findings of Fyfe and Flato (1999) for the Rocky Mountains. Regarding precipitation, our results for the Alpine region differ from that of Giorgi et al. The latter, for instance, found an increase of precipitation sums in most seasons and at most altitudes, while our analysis suggests dryer conditions especially during summer and at low elevations. However, the simulated precipitation changes are in most regions not significant (see Fig. 7). Furthermore, differences between the two studies could be explained by the different model setup (5- and 3-year time slices vs. 30-year time slices; $2xCO_2$ equilibrium run vs. transient A1B run; 50 km horizontal resolution vs. 25 km; driving GCM) and especially by differences in the convective parameterization scheme employed, with the latter still representing a major source of uncertainty in climate modeling (e.g., Brockhaus 2009, Hohenegger et al. 2009).

6 Conclusions

The present study provides a European-scale overview on possible elevation dependencies of 21st century near-surface climate change. Our analysis of a COSMO-CLM transient climate change experiment suggests that future climate change might considerably depend on surface elevation over most parts of Europe and in most seasons. For 2 m temperature, the general picture is an intensification of the projected warming with elevation, which becomes apparent during the first half of the 21st century and which results in a general

decrease of surface lapse rates. The amplification of the large-scale warming at high elevations is partly connected to well-known large-scale processes in the free troposphere. These are controlled by changes in moist-adiabatic lapse rates, imply an increase in dry atmospheric stability, and ultimately lead to the water-vapor-lapse-rate feedback (e.g., Soden and Held 2006). In our modeling framework, these large-scale changes stem from the driving global model. In addition, large-scale land-sea contrasts (along with different warming rates over land and sea) contribute to gradients in the warming signal in regions with a significant fraction of coast lines. The mentioned large-scale influences are strongly modulated or even dominated by local and regional-scale processes involving the land surface. In winter and spring the anomalously large high-elevation warming is connected to a decrease in snow cover, suggesting a contribution of the snow-albedo feedback mechanism. In some regions, the same is true for summer and autumn. Further factors include elevation-dependent changes in cloud cover and soil moisture as well as the proximity of low-elevation regions to the sea. For precipitation, only few consistent altitudinal signals valid for several regions arise and typically only changes in summer precipitation are found to be significant.

The horizontal resolution applied in our study (about 25 km) allows representing climatic details on a regional scale, but still considerably smoothes the real topography. This leaves the question whether the simulated elevation gradients of climate change could be extrapolated to elevations higher than the maximum grid cell elevation in a certain region, for instance to places above 2700 m in the European Alps. Figure 5 (2 m temperature) and 7 (precipitation) would suggest such a possibility. But as long as snow cover changes can be identified as a governing process, which is mostly the case for 2 m temperature elevation gradients, we would not recommend any such extrapolation. The non-linear character of the processes involved in snow accumulation and ablation and the dependency of surface snow cover on both temperature and precipitation could lead to high-altitude snow cover changes which are inconsistent to those found at lower elevations. In the case of the Alps, the simulated increase of winter precipitation could offset temperature effects beyond a certain altitude, resulting in a less pronounced decrease or even an increase in the number of snow days and, hence, a less pronounced amplification of the large-scale warming via the snow-albedo feedback. Updated CCLM scenarios at higher resolution carried out within the CORDEX initiative (*Coordinated Regional Climate Downscaling Experiment*; Giorgi et al. 2009) can be expected to give new insight into climatic changes occurring at elevations above the currently resolved range.

The present study has a number of limitations. An obvious source of uncertainty is that we only applied one individual RCM driven by one individual GCM. Different results might be obtained for different model combinations. The model agreement/disagreement on the elevation signal of climate change will be the subject of a subsequent study analyzing the full set of ENSEMBLES RCMs. Further uncertainties relate to future land cover changes which are not considered in the CCLM experiment analyzed here. In case that such changes correlate with elevation, they would introduce an additional elevation-dependent forcing and could alter the elevation gradients of near-surface climate change. For instance, in addition to snow processes, selected regions in the Alps, Scandinavia and partly also in the Pyrenees might be affected by 21st century glacier retreat and its impacts on land surface albedo (replacement of brighter ice surfaces by bare rock/gravel; ice-albedo feedback) and surface temperature (replacement of ice surfaces with a maximum surface temperature of 0°C by bare rock/gravel with higher surface temperatures possible). These processes are not yet accounted for in CCLM but might additionally amplify temperature changes at high elevations during summer (i.e., after the seasonal snow cover has melted).

Similar concerns relate to future changes in aerosol characteristics which are not accounted for but which could introduce an elevation-dependent effect as well. Further aspects that require a thorough investigation are the effects of natural climate variability and the influence of the greenhouse gas emission scenario assumed.

Despite the mentioned uncertainties, our analysis clearly indicates a possible elevation-dependency of future European climate change. A robust and physically plausible feature is the amplification of the anticipated temperature change at high elevations. This result has important implications for a number of further disciplines and applications. In particular studies that are dealing with possible impacts of climate change in mountainous regions with their pronounced topographic variability would profit from taking into account the elevation dependency of near-surface climate change. Given, for instance, the pronounced difference of seasonal temperature changes between low and high-elevation regions in many parts of Europe, assuming a uniform temperature change would be too simplistic for assessing the response of temperature-dependent systems to climate change (e.g., snow cover, hydrology, ecosystems). These examples highlight that the implications of an elevation-dependent climatic forcing can be manifold and require further interdisciplinary study. In particular, the amplified warming at high elevations will challenge the adaptability of both natural and anthropogenic high-altitude systems to climate change.

Acknowledgements The COSMO-CLM simulations analyzed have been conducted at the Swiss National Supercomputing Centre (CSCS). We are indebted to the COSMO and CLM communities for providing access to and support for the model, as well as to MeteoSwiss and ECMWF for providing access to the ERA40 data set. The ENSEMBLES data used in this work was funded by the EU FP6 Integrated Project ENSEMBLES (Contract number 505539) whose support is gratefully acknowledged. We also acknowledge the E-OBS dataset from the ENSEMBLES project and the data providers in the ECA&D project (http://eca.knmi.nl). Partial funding for this study has been provided by the Swiss National Science Foundation via NCCR Climate. We are thankful to the Center for Climate Systems Modeling (C2SM) for modeling support and to Dr. Tracy Ewen for her valuable input.

References

Adam JC, Lettenmaier DP (2003) Adjustment of global gridded precipitation for systematic bias. J Geophys Res 108(D9):4257. doi:10.1029/2002JD002499

Appenzeller C, Begert M, Zenklusen E, Scherrer SC (2008) Monitoring climate at Jungfraujoch in the high Swiss Alpine region. Science Tot Env 391:262–268

Barry RG (2008) Mountain Weather and Climate. 3 rd edn, Cambridge University Press

Beniston M, Rebetez M (1996) Regional behavior of minimum temperatures in Switzerland for the period 1979–1993. Theor Appl Climatol 53:231–243

Beniston M, Diaz HF, Bradley RS (1997) Climatic change at high elevation sites: an overview. Clim Change 36:233–251

Brockhaus P (2009) Role and representation of moist convection in a regional climate model. PhD thesis. Swiss Federal Institute of Technology (ETH) Zurich, Diss. ETH No. 18624, 144 pp

Ceppi P, Scherrer SC, Fischer AM, Appenzeller C (2010) Revisiting Swiss temperature trends 1959–2008. Int J Clim, accepted. doi:10.1002/joc.2260

Christensen JH, Carter TR, Rummukainen M, Amanatidis G (2007) Evaluating the performance and utility of regional climate models: the PRUDENCE project. Clim Change 81:1–16. doi:10.1007/s10584-006-9211-6

Christensen JH, Christensen OB (2007) A summary of the PRUDENCE model projections of changes in European climate by the end of this century. Clim Change 81:7–30. doi:10.1007/s10584-006-9210-7

Daly C, Neilson RP, Phillips DL (1994) A statistical-topographic model for mapping climatological precipitation over mountainous terrain. J Appl Meteorol 33:140–158

Davies HC (1976) A lateral boundary formulation for multi-level prediction models. Q J Roy Meteor Soc 102:405–418
Diaz HF, Bradley RS (1997) Temperature variations during the last century at high elevation sites. Clim Change 36:253–279
Diaz HF, Grosjean M, Graumlich L (2003) Climate variability and change in high elevation regions: past, present and future. Clim Change 59:1–4
Durand Y, Giraud G, Laternser M, Etchevers P, Mérindol L, Lesaffre B (2009) Reanalysis of 47 years of climate in the french Alps (1958–2005): climatology and trends for snow cover. J Appl Meteorol Climatol 48:2487–2512. doi:10.1175/2009JAMC1810.1
EEA (2009) Regional climate change and adaptation – The Alps facing the challenge of changing water resources. European Environment Agency Report No. 8/2009, Copenhagen, 143 pp
Elsasser H, Bürki R (2002) Climate change as a threat to tourism in the Alps. Clim Res 20:253–257
Frei C, Schär C (1998) A precipitation climatology of the Alps from high-resolution rain-gauge observations. Int J Climatol 18:873–900
Frei C, Davies HC, Gurtz J, Schär C (2000) Climate dynamics and extreme precipitation and flood events in central Europe. Integr Assess 1:281–299
Frierson DMW (2006) Robust increases in midlatitude static stability in simulations of global warming. Geophys Res Lett 33:L24816. doi:10.1029/2006GL027504
Fyfe JC, Flato GM (1999) Enhanced climate change and its detection over the rocky mountains. J Clim 12:230–243
Giorgi F, Hurrell JW, Marinucci MR (1997) Elevation dependency of the surface climate change signal: a model study. Clim Change 10:288–296
Giorgi F, Jones C, Asrar GR (2009) Addressing climate information needs at the regional level: the CORDEX framework. WMO Bull 58(3):175–183
Gordon C, Cooper C, Senior CA, Banks H, Gregory JM, Johns TC, Mitchell JFB, Wood RA (2000) The simulation of SST, sea ice extents and ocean heat transports in a version of the Hadley Centre coupled model without flux adjustments. Clim Dyn 16:147–168
Hall A (2004) The role of surface Albedo feedback in climate. J Clim 17:1550–1568
Hantel M, Ehrendorfer M, Haslinger A (2000) Climate sensitivity of snow cover duration in Austria. Int J Climatol 20:615–640
Haylock MR, Hofstra N, Klein Tank AMG, Klok EJ, Jones PD, New M (2008) A European daily high-resolution gridded data set of surface temperature and precipitation for 1950–2006. J Geophys Res 113: D20119. doi:10.1029/2008JD010201
Held IM, Soden BJ (2000) Water vapor feedback and global warming. Annu Rev Energy Environ 25:441–475
Hiebl J, Auer I, Böhm R, Schöner W, Maugeri M, Lentini G, Spinoni J, Brunetti M, Nanni T, Tadić MP, Bihari Z, Dolinar M, Müller-Westermeier G (2009) A high-resolution 1961–1990 monthly temperature climatology for the greater Alpine region. Meteorol Z 18(5):507–530. doi:10.1127/0941-2948/2009/0403
Hohenegger C, Brockhaus P, Bretherton CS, Schär C (2009) The soil moisture–precipitation feedback in simulations with explicit and parameterized convection. J Clim 22:5003–5020
Houze RA (1993) Cloud Dynamics. Academic Press, San Diego. International Geophysics Series, Volume 53, 570 pp
Im E-S, Coppola E, Giorgi F, Bi X (2010) Local effects of climate change over the Alpine region: A study with a high resolution regional climate model with a surrogate climate change signal. Geophys Res Lett 37:L05704. doi:10.1029/2009GL041801
IPCC (2007) Climate Change 2007: The Physical Science Basis. Contribution of Working Group I to the Fourth Assessment Report of the Intergovernmental Panel on Climate Change. Cambridge University Press, Cambridge, UK and New York, NY, USA, 996 pp
Jaeger EB, Anders I, Lüthi D, Rockel B, Schär C, Seneviratne S (2008) Analysis of ERA40-driven CLM simulations for Europe. Meteorol Z 17(4):1–19. doi:10.1127/0941-2948/2008/0301
Kim J (2001) A nested modeling study of elevation-dependent climate change signals in California induced by increased atmospheric CO_2. Geophys Res Lett 28(15):2951–2954
Kotlarski S, Block A, Böhm U, Jacob D, Keuler K, Knoche R, Rechid D, Walter A (2005) Regional climate model simulations as input for hydrological applications: evaluation of uncertainties. Adv Geosciences 5:119–125
Kotlarski S, Paul F, Jacob D (2010) Forcing a distributed glacier mass balance model with the regional climate model REMO, part I: climate model evaluation. J Clim 23(6):1589–1606. doi:10.1175/2009JCLI2711.1
Laternser MC (2002) Snow and avalanche climatology of Switzerland. PhD thesis. Swiss Federal Institute of Technology (ETH) Zurich, Diss. ETH No. 14493, 137 pp

Leung LR, Ghan SJ (1999) Pacific northwest climate sensitivity simulated by a regional climate model driven by a GCM. Part II: 2xCO_2 simulations. J Clim 12:2031–2053

López-Moreno JI, Goyette S, Beniston M (2008) Climate change prediction over complex areas: spatial variability of uncertainties and predictions over the Pyrenees from a set of regional climate models. Int J Climatol 28:1535–1550

Marty C, Philipona R, Fröhlich C, Ohmura A (2002) Altitude dependence of surface radiation fluxes and cloud forcing in the alps: results from the alpine surface radiation budget network. Theor Appl Climatol 72:137–155

Minder JR, Mote PW, Lundquist JD (2010) Surface temperature lapse rates over complex terrain: Lessons from the Cascade Mountains. J Geophys Res 115:D14122. doi:10.1029/2009JD013493

Nakicenovic N, Alcamo J, Davis G, de Vries B, Fenhann J, Gaffin S, Gregory K, Grübler A, Yong Jung T, Kram T, Lebre La Rovere E, Michaelis L, Mori S, Morita T, Pepper W, Pitcher H, Price L, Riahi K, Roehrl A, Rogner H-H, Sankovski A, Schlesinger M, Shukla P, Smith S, Swart R, van Rooijen S, Victor N, Dadi Z (2000) Special Report on Emissions Scenarios: A Special Report of Working Group III of the Intergovernmental Panel on Climate Change. Cambridge University Press, Cambridge, UK, p 599

Pepin N, Losleben M (2002) Climate change in the Colorado rocky mountains: free air versus surface temperature trends. Int J Climatol 22:311–329. doi:10.1002/joc.740

Prömmel K, Geyer B, Jones JM, Widmann M (2010) Evaluation of the skill and added value of a reanalysis-driven regional simulation for Alpine temperature. Int J Climatol 30:760–773. doi:10.1002/joc.1916

Richner H, Phillips PD (1984) A comparison of temperature from mountaintops and the free atmosphere – their diurnal variation and mean difference. Mon Weather Rev 112(7):1328–1340

Ritter B, Geleyn J-F (1992) A comprehensive radiation scheme for numerical weather prediction models with potential applications in climate simulations. Mon Weather Rev 120:303–325

Rockel B, Will A, Hense A (2008) The regional climate model COSMO-CLM (CCLM). Meteorol Z 17 (4):347–348. doi:10.1127/0941-2948/2008/0309

Roe GH (2005) Orographic precipitation. Annu Rev Earth Planet Sci 33:645–671. doi:10.1146/annurev.earth.33.092203.122541

Rolland C (2003) Spatial and seasonal variations of air temperature lapse rates in Alpine regions. J Clim 16:1032–1046

Salathé EP, Leung LR, Qian Y, Zhang Y (2010) Regional climate model projections for the State of Washington. Clim Change 102:51–75. doi:10.1007/s10584-010-9849-y

Santer BD et al (2005) Amplification of surface temperature trends and variability in the tropical atmosphere. Science 309:1551–1556. doi:10.1126/science.1114867

Schär C, Frei C, Lüthi D, Davies HC (1996) Surrogate climate-change scenarios for regional climate models. Geophys Res Lett 23:669–672. doi:10.1029/96GL00265

Schär C, Davies TD, Frei C, Wanner H, Widmann M, Wild M, Davies HC (1998) Current Alpine Climate. In: Cebon P, Dahinden U, Davies HC, Imboden DM, Jäger CC (eds) Views from the Alps: Regional perspectives on climate change. MIT Press, Boston, pp 21–72

Schröter D et al (2005) Ecosystem service supply and vulnerability to global change in Europe. Science 310 (5752):1333–1337. doi:10.1126/science.1115233

Schwarb M (2000) The Alpine Precipitation Climate—Evaluation of a high-resolution analysis scheme using comprehensive rain-gauge data. PhD thesis. Swiss Federal Institute of Technology (ETH) Zurich, Diss. ETH No. 13911, 131 pp

Schwarb M, Daly C, Frei C, Schär C (2001) Mean annual and seasonal precipitation throughout the European Alps 1971–1990. In: Hydrological Atlas of Switzerland. Plates 2.6 and 2.7. Swiss Federal Office for Water and Geology, Bern

Seidel DJ, Free M (2003) Comaprison of lower-tropospheric temperature climatologies and trends at low and high elevation radiosonde sites. Clim Change 59:53–74

Sevruk B (1997) Regional dependency of the precipitation-altitude relationship in the Swiss Alps. Clim Change 36:355–369

Smith RB (1979) The influence of mountains on the atmosphere. Adv Geophys 21:87–230

Snyder MA, Bell JL, Sloan LC, Duffy PB, Govindasamy B (2002) Climate responses to a doubling of atmospheric carbon dioxide for a climatically vulnerable region. Geophys Res Lett 29(11):9. doi:10.1029/2001GL014431

Snyder MA, Sloan LC (2005) Transient future climate over the Western United States using a regional climate model. Earth Interact 9:1–21

Soden BJ, Held IM (2006) An assessment of climate feedbacks in coupled ocean-atmosphere models. J Clim 19:3354–3360

Steppeler J, Doms G, Schättler U, Bitzer H, Gassmann A, Damrath U, Gregoric G (2003) Meso-gamma scale forecasts using the nonhydrostatic model LM. Meteor Atmos Phys 82:75–96

Thuiller W, Lavorel S, Araujo MB, Sykes MT, Prentice IC (2005) Climate change threats to plant diversity in Europe. PNAS 102(23):8245–8250. doi:10.1073/pnas.0409902102

Tiedtke M (1989) A comprehensive mass flux scheme for cumulus parameterization in large-scale models. Mon Weather Rev 117:1779–1799

Uppala SM, Kallberg PW, Simmons AJ, Andrae U, da Costa BV, Fiorino M, Gibson JK, Haseler J, Hernandez A, Kelly GA, Li X, Onogi K, Saarinen S, Sokka N, Allan RP, Andersson E, Arpe K, Balmaseda MA, Beljaars ACM, van de Berg L, Bidlot J, Bormann N, Caires S, Chevallier F, Dethof A, Dragosavac M, Fisher M, Fuentes M, Hagemann S, Holm E, Hoskins BJ, Isaksen L, Janssen PAEM, Jenne R, McNally AP, Mahfouf J-F, Morcrette J-J, Rayner NA, Saunders RW, Simon P, Sterl A, Trenberth KE, Untch A, Vasiljevic D, Viterbo P, Woollen J (2005) The ERA-40 re-analysis. Q J Roy Meteor Soc 131:2961–3012

van der Linden P, Mitchell JFB (2009) ENSEMBLES: Climate Change and its Impacts: Summary of research and results from the ENSEMBLES project. Met Office Hadley Centre, FitzRoy Road, Exeter EX1 3 PB, UK. 160 pp

Varney BM (1920) Monthly variations of the precipitation-altitude relation in the Central Sierra Nevada of California. Mon Weather Rev 48(11):648–650

Verbunt M, Walser A, Gurtz J, Montani A, Schär C (2007) Probabilistic flood forecasting with a limited-area ensemble prediction system. J Hydrometeorol 8(4):897–909

Vidale PL, Lüthi D, Frei C, Seneviratne SI, Schär C (2003) Predictability and uncertainty in a regional climate model. J Geophys Res 108(D18):4586. doi:10.1029/2002JD002810

Viviroli D, Dürr HH, Messerli B, Meybeck M, Weingartner R (2007) Mountains of the world, water towers for humanity: Typology, mapping, and global significance. Water Resour Res 43(7):W07447. doi:10.1029/2006WR005653

Vuille M, Bradley RS (2000) Mean annual temperature trends and their vertical structure in the tropical Andes. Geophys Res Lett 27(23):3885–3888

Wastl C, Zängl G (2007) Analysis of the climatological precipitation gradient between the Alpine foreland and the northern Alps. Met Z 16(5):541–552

Wastl C, Zängl G (2008) Analysis of mountain-valley precipitation differences in the Alps. Met Z 17(3):311–321

Weber RO, Talkner P, Stefanicki G (1994) Asymetric diurnal temperature change in the Alpine region. Geophys Res Lett 21(8):673–676

Weber RO, Talkner P, Auer I, Böhm R, Gajić-Čapka M, Zaninović K, Brázdil R, Faško P (1997) 20th-Century changes of temperature in the mountain regions of central Europe. Clim Change 36:327–344

Weischet W (1979) Einführung in die Allgemeine Klimatologie, 2nd edn. Teubner, Stuttgart

Wild M, Ohmura A, Cubasch U (1997) GCM-simulated surface energy fluxes in climate change experiments. J Clim 10:3093–3110

Wilks DS (2006) Statistical Methods in the Atmospheric Sciences. Second Edition. International Geophysics Series Vol. 91. Elsevier Inc., 627 pp

You Q, Kang S, Pepin N, Flügel W-A, Yan Y, Behrawan H, Huang J (2010) Relationship between temperature trend magnitude, elevation and mean temperature in the Tibetan Plateau from homogenized surface stations and reanalysis data. Glob Planet Change 71:124–133. doi:10.1016/j.gloplacha.2010.01.020